Effects of Sugars, Furans, and their Derivatives on Hydrodeoxygenation of Biorefinery Lignin-Rich Wastes to Hydrocarbons

Hongliang Wang,[a, b] Yuhua Duan,[d] Qian Zhang,[e] and Bin Yang*[a, c]

Hydrodeoxygenation of biorefinery lignin-rich wastes to jet fuel hydrocarbons offers a significant opportunity for enhancing the overall operational efficiency, carbon conversion efficiency, economic viability, and sustainability of biofuels production. However, these wastes usually mainly contain lignin with sugars, furans, and their derivatives as "impurities". Although several factors, including reactant structure, solvents, or the decreased ratio of catalyst to reactant, could be responsible for the jet fuel hydrocarbons yield loss, we found evidence that glucose, xylose, and 5-hydroxymethylfurfural dramatically decreased conversion yields. For example, xylose and glucose lowered the final hydrocarbon yield by 78 and 63%, respectively. The results revealed that these compounds could suppress metal catalysts and inhibit lignin depolymerization and hydrodeoxygenation (HDO) reactions thus decrease yields of jet fuel range hydrocarbons from biomass-derived lignin. The first-principles calculations and TGA results from spent catalysts validated these findings.

Introduction

Efficient utilization of all available carbons from biomass to produce biofuels will be required for an economical process. Catalytic technologies for conversion of biorefinery wastes at high carbon efficiency for maximal biofuel production are critical for enabling a robust biorefinery industry.[1–3] Biorefinery lignin-rich wastes are the partially dewatered stream containing lignin as well as unconverted biomass components such as sugars, furans, and their derivatives. Such wastes are often burned to supply self-sustaining energy to the biorefinery or discarded. However, the chemical structure of lignin suggest that it not only can be used to produce energy, but also has great potential for production of value-added fuels and chemicals.[4–8] Unlike conversion of carbohydrates into biofuels,[4–7] effective conversion of lignin and lignin-rich biorefinery wastes remains challenging.[8–10] If the US replaces 25% of transportation fuels with biofuels by 2030, it will produce around 50 billion gallons of cellulosic ethanol and up to 0.3 billion tons of resultant lignin. The amount of lignin wastes will substantially exceed the power demand of the biorefinery operation. Efforts are critically needed to transform lignin-rich wastes into higher value products. Lignin depolymerization and subsequent HDO conversion into hydrocarbons under catalytic conditions is one of the most promising approaches for its rational utilization.[8,9] The catalytic efficiency as well as the generated products (yield, composition, and distribution) of lignin HDO approach can be regulated by several important factors, such as catalysts, hydrogen pressure, solvents, trapping agents, reaction temperature, and time.[7,11–14] Extensive research work on these aspects has been conducted to fully unlock lignin's potential.[15–17] Effects of lignin characteristics, including its origins (softwood, hardwood, or herbaceous plant), molecular weight, and chemical linkages, on its HDO conversion also have been extensively studied.[10,17–21] However, relatively few studies have been devoted to the determination of effects of impurities (e.g., sugar, furans, and their derivatives) in lignin-rich wastes on its HDO conversion.

Lignin from biorefinery processes always contains some impurities. The majority of these impurities are carbohydrates (sugars) or other derivatives of cellulose and hemicellulose.[21,22] Potential effects of sugars, furans, and their derivatives on lignin HDO conversion, including adsorption onto catalysts, reacting with lignin and its degraded intermediates, remain unexplored. In this study, to simulate real lignin degraded intermediates, lignin model compounds were mixed with various sugars to investigate effects of sugars on the HDO conversion of lignin, including on the product compositions and distribution, the efficiency of breaking different C—O—C bonds among

[a] Dr. H. Wang, Prof. B. Yang
Department of Biological Systems Engineering
Washington State University, Richland, WA 99354 (USA)
E-mail: bin.yang@wsu.edu

[b] Dr. H. Wang
Center of Biomass Engineering/College of Agronomy and Biotechnology
China Agricultural University, Beijing, 100193 (China)

[c] Prof. B. Yang
Earth and Biological Sciences Directorate
Pacific Northwest National Laboratory, Richland, WA 99352 (USA)
E-mail: bin.yang@pnnl.gov

[d] Dr. Y. Duan
National Energy Technology Laboratory
United States Department of Energy, Pittsburgh, PA 15236 (USA)

[e] Dr. Q. Zhang
Key Laboratory of Coal Science and Technology of Ministry of Education
and Shanxi Province, Taiyuan University of Technology
Taiyuan, 030024, Shanxi (China)

[iD] The ORCID identification number(s) for the author(s) of this article can be found under:
https://doi.org/10.1002/cssc.201801401.

lignin interlinkages. Subsequently, to get more insights into effects of sugars on real lignin HDO conversion, HDO reactions of lignin mixed with two typical monosaccharides (i.e., glucose and xylose) were investigated. The lignin used in this study was prepared from dilute alkali deacetylation and mechanical refining (DMR) treatment, a biomass deconstruction process developed at the National Renewable Energy Laboratory (NREL).[23] The catalyst system used here was a combination of a super Lewis acid In(OTf)$_3$ with an inexpensive noble metal-based catalyst (Ru/Al$_2$O$_3$). It was reported that lignin and its phenol derivatives were successfully converted by the combination of metallic and acidic functions.[24] Indium triflate is an environmentally friendly, inexpensive, reusable, and water-tolerant Lewis acid.[25] More importantly, it has shown high activity in hydrolysis of lignin and its model compounds.[24–27] Ruthenium-based catalysts have been widely used in lignin HDO conversion, exhibiting high deoxygenation and hydrogenation activities in aqueous solution.[26–29]

Results and Discussion

Initially in this study, guaiacol was selected as a lignin model compound for the investigation of effects of carbohydrates and their derivatives (i.e., glucose, xylose, 5-HMF, cellulose) on lignin HDO conversion. Six types of HDO main products were detected (Table 1). Product type **6** consisted mainly of alkylphenols and alkylcyclohexanols. Although addition of 10 mol% glucose in the reactant did not significantly change the amount of guaiacol converted, it strongly affected the product distribution. The selectivity of the primary product (product **1**, 1,2-benzenediol) with 10 mol% glucose addition was much higher than that with pure guaiacol as reactant (Table 1, entries 1 and 2). Meanwhile, without addition of any sugars, the selectivity of aromatic ring hydrogenated products (products **3**–**5**) was moderate. However, with the addition of 10 mol% glucose, the selectivity to these products became fairly low. These results indicated that the presence of glucose had significant effects on the further conversion of 1,2-benzenediol into aromatic ring-saturated products, although it showed little effect on the conversion of guaiacol into 1,2-benzenediol.

Because both In(OTf)$_3$ and Ru/Al$_2$O$_3$ can catalyze the conversion of guaiacol into 1,2-benzenediol, but only Ru/Al$_2$O$_3$ can catalyze the conversion of 1,2-benzenediol into products **3**–**5**, the inhibition of 1,2-benzenediol conversion into aromatic ring-saturated products in Table 1, entry 2 is likely due to the deactivation of Ru/Al$_2$O$_3$ by glucose or its derivatives. To test this hypothesis, In(OTf)$_3$ and Ru/Al$_2$O$_3$ were tested separately. Results showed that when In(OTf)$_3$ was used alone, the addition of 10 mol% of glucose to the reactants had little effect on either guaiacol conversion or product distribution. 1,2-Benzenediol was found to be the dominant product with both catalysts. When the glucose content was increased to 30 mol%, the guaiacol conversion slightly decreased 3.9%. On further increasing the glucose content to 60 mol%, the guaiacol conversion dropped by 14.4%. These results suggested that glucose had little effect on the acidic conversion of guaiacol. However, under the catalysis of Ru/Al$_2$O$_3$, both guaiacol conversion and product distribution changed significantly on the addition of glucose. The conversion of guaiacol decreased from 79% to 55% when 10 mol% glucose was added. Further increase of the glucose content to 30 mol% led to a sharp decrease in the guaiacol conversion to 30%. Meanwhile, the selectivity to aromatic ring-saturated products dropped significantly when glucose was added (Table 1, entries 8 and 9).

To evaluate the influence of other common carbohydrates or their derivatives on guaiacol HDO conversion under Ru/Al$_2$O$_3$ catalysis, xylose, 5-hydroxymethylfurfural (HMF), and cel-

Table 1. HDO conversion of guaiacol with carbohydrates and their derivatives.[a]

Entry	Catalyst	Carbohydrate	Conversion [wt%]	Product selectivity [C%]					
				1	2	3	4	5	6
1	In(OTf)$_3$ + Ru/Al$_2$O$_3$	–	72.5	26.1	10.3	15.1	22.4	22.6	3.5
2	In(OTf)$_3$ + Ru/Al$_2$O$_3$	glucose (0.1 mmol)	68.2	55.2	14.2	4.6	8.7	7.6	9.7
3	In(OTf)$_3$	–	65.6	85.3	12.6	N.R.	N.R.	N.R.	2.1
4	In(OTf)$_3$	glucose (0.1 mmol)	64.9	88.9	8.2	N.R.	N.R.	N.R.	2.9
5	In(OTf)$_3$	glucose (0.3 mmol)	61.7	90.5	5.0	N.R.	N.R.	N.R.	4.5
6	In(OTf)$_3$	glucose (0.6 mmol)	51.2	94.5	3.7	N.R.	N.R.	N.R.	1.8
7	Ru/Al$_2$O$_3$	–	79.3	10.2	6.7	26.7	17.4	30.5	8.5
8	Ru/Al$_2$O$_3$	glucose (0.1 mmol)	55.3	36.8	15.3	11.9	16.6	14.1	5.3
9	Ru/Al$_2$O$_3$	glucose (0.3 mmol)	30.1	48.2	10.7	9.0	11.3	10.3	10.5
10	Ru/Al$_2$O$_3$	xylose (0.1 mmol)	48.6	39.9	16.1	9.8	17.1	11.0	6.1
11	Ru/Al$_2$O$_3$	5-HMF (0.1 mmol)	41.7	45.3	18.9	7.5	9.3	9.5	9.5
12	Ru/Al$_2$O$_3$	cellulose (0.1 mmol)	64.1	28.3	11.9	19.6	14.5	23.6	2.1
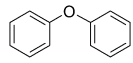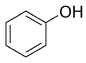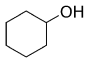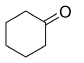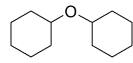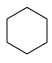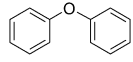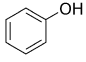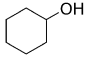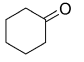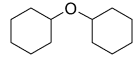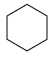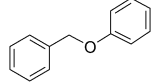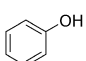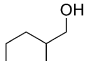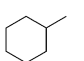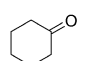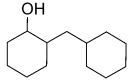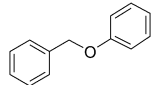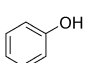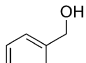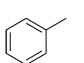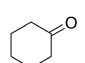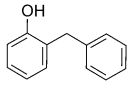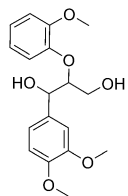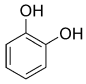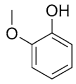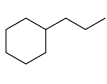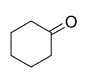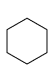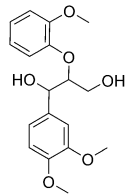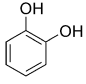
[a] Reaction conditions: $n_{\text{guaiacol}} + n_{\text{carbohydrate}} = 1$ mmol, In(OTf)$_3$ (0.05 mmol), Ru (0.025 mmol) as 5 wt% Ru/Al$_2$O$_3$, water (1 mL), $T = 250\,°C$, $t = 2$ h, $P_{\text{H}_2} = 580$ psi. N.R. indicates that no product was detected.

lulose were mixed separately with guaiacol under identical reaction conditions, (Table 1, entries 10–12). Both xylose and HMF significantly suppressed the catalytic activity of Ru/Al₂O₃. The addition of cellulose also decreased the HDO catalytic activity of Ru/Al₂O₃ although not as strongly as the monosaccharides or HMF. Results showed that the inhibition by carbohydrates on Ru/Al₂O₃ decreased as follows: 5-HMF > xylose > glucose > cellulose. This sequence appears to be in line with the amount of products containing the aromatic furan ring that formed from those carbohydrates under the reaction conditions. HMF is a dehydration product of hexose and a furan-based compound, which can compete with guaiacol to adsorb onto the surface of ruthenium nanoparticle and thus suppress the HDO conversion of guaiacol.[18] Xylose comes from hemicellulose, and it can be easily converted into furfural (also contains an aromatic furan ring) under hydrothermal or acidic conditions. Compared with xylose, glucose and cellulose are more difficult to convert into furan-based compounds. Meanwhile, previous studies also reported the suppression of catalytic hydrogenation activities of metals by furan compounds.[21, 22, 30]

In addition to the conversion of guaiacol, the effects of sugars on the HDO conversion of several lignin dimers, which contain typical ether linkages of lignin and are usually generated during lignin HDO, were further explored to provide more fundamental insights into sugar effects on lignin HDO. Since β-O-4, α-O-4, 4-O-5 bonds are the most abundant C—O—C bonds in lignin linkages, diphenyl ether (DPE), benzyl phenyl ether (BPE), and veratrylglycero-β-guaiacyl ether (VGE; Table 2) were chosen to represent aryl—O—aryl (4-O-5), aryl—O—benzyl (α-O-4), and aryl—O—alkyl (β-O-4) linkages, respectively, to test effects of sugars on the breakage of a wide range of C—O—C bonds under lignin HDO conversion conditions. These model compounds cover various C—O bond strengths in lignin, typically with bond dissociation enthalpy (BDE): 4-O-5 > α-O-4 > β-O-4. The conversion of these model compounds and the selectivity of their top five products are listed in Table 2.

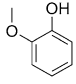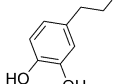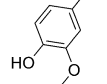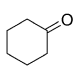HDO conversion of DPE was 56.3 % and the yield of aromatic ring hydrogenated products was 24 % (Table 2). The moderate conversion of DPE under the reaction conditions was probably due to the high bond dissociation enthalpy of the 4-O-5 ether

Table 2. HDO conversion of lignin dimers over the combined catalysis of In(OTf)₃ and Ru/Al₂O₃.[a]

| Entry	Reactant	Conversion [wt%]	Selectivity [C%]				
1	DPE	56.3	55.3	11.7	25.4	3.1	1.9
2[b]	DPE	36.8	80.3	7.4	8.2	2.6	0.8
3	BPE	>99	33.9	27.1	14.7	11.3	8.6
4[b]	BPE	84.6	41.0	19.6	21.0	9.7	6.3
5	VGE	>99	27.4	18.4	16.9	15.4	11.8
6[b]	VGE	78.6	33.6	15.1	18.3	14.5	9.1

Reaction conditions: In(OTf)₃ (0.05 mmol), Ru (0.025 mmol) as 5 wt% Ru/Al₂O₃, water (1 mL), T = 250 °C, t = 2 h, P$_{H_2}$ = 580 psi. [a] Guaiacol (1 mmol). [b] Guaiacol (0.9 mmol), glucose (0.1 mmol).

bond. DPE conversion dropped to about 37% when 10 mol% glucose was added. At the same time, the selectivity to aromatic ring-hydrogenated products significantly decreased. Since the α-O-4 ether bond has a relatively low bond dissociation enthalpy, complete conversion of BPE was achieved when no sugar was added. However, when 10 mol% of glucose was added, the conversion of BPE decreased to about 85%. The addition of glucose also changed the distribution of BPE HDO products. The selectivity to partially hydrogenated products (aromatics) significantly increased from 34 to 88% when glucose was added. Similar results were obtained from HDO conversion of VGE with the β-O-4 bond, the most prevalent ether bond in lignin interlinkages. The presence of glucose not only decreased the VGE conversion but also lowered the selectivities of deoxygenated and fully hydrogenated products. Results obtained from HDO conversion of lignin dimers with glucose were consistent with those obtained from HDO conversion of guaiacol, revealing that sugars affected the hydrogenolysis and hydrogenation activities of the catalysis system.

In addition, effects of sugars (glucose or xylose) on HDO conversion of technical lignin were investigated. The conversion of lignin and the total yield of products are shown in Figure 1a and the generated GC-MS detectable products are shown in Figure 1b. Results showed that the addition of 10 wt% sugars (either glucose or xylose) significantly hindered HDO conversion of lignin, and they showed greater effects on lignin than on lignin model compounds. Compared to the conversion of lignin model compounds, the conversion of technical lignin decreased more rapidly after sugars were added. The macromolecular form of technical lignin that is disadvanta-

geous in the competitive adsorption on the metal catalyst can be the primary cause for the loss in hydrocarbons yield from HDO of technical lignin although several factors, including reactant structure, solvents, or the decreased ratio of catalyst to reactant, can be responsible. Furthermore, xylose was more inhibitory than glucose in terms of decreasing hydrocarbon yield. Xylose and glucose lowered the final hydrocarbon yield by 78% and 63%, respectively. Moreover, we found the color of the ethyl acetate extract with the addition of sugar was quite different from that without sugar (Figure 1c). The ethyl acetate extract of products from lignin without added sugars appeared faint yellow. In contrast, with the addition of sugars, the ethyl acetate extract of products was brownish black. This is probably due to the production of humins from the added sugars under the reaction conditions. Humins can also adsorb on the catalyst surface and thus decrease its catalytic activity.

Based on the obtained results, a potential mechanism of the effects of carbohydrates and their derivatives on lignin conversion over catalysis of Ru/Al$_2$O$_3$ is proposed (Scheme 1). Furan-
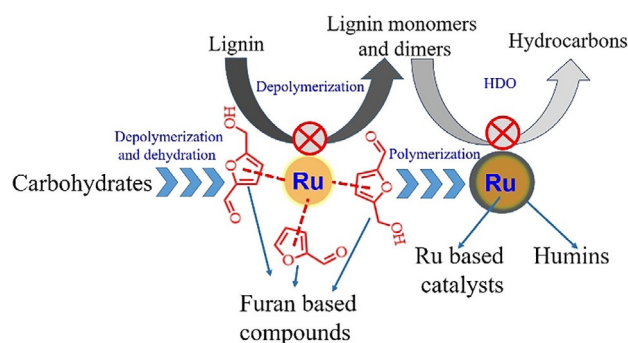
Scheme 1. Proposed mechanism of carbohydrate effects on lignin depolymerization and HDO conversion over Ru/Al$_2$O$_3$ catalyst.

based compounds, including 5-HMF and furfural generated from carbohydrates through depolymerization and dehydration, competitively adsorb on the Ru metal particles with lignin and thus prevent lignin from hydrogenolysis depolymerization. The adsorption of furan-based compounds on Ru also hinders HDO conversion of depolymerized lignin intermediates. Moreover, humins formed by the polymerization of furan-based compounds and other carbohydrate derivatives could cover the Ru particle surface and thus deactivate the metal catalyst.

To test the proposed mechanism (Scheme 1), we performed first-principles density functional theory (DFT) calculations on molecules produced from carbohydrates (furfural, 5-HMF, levulinic acid) and from lignin (guaiacol, phenol, cresol) adsorbed on the Ru (0001) surface. The obtained adsorption energies (E_{ads}) of these molecules, as well as two example adsorption configurations, are shown in Figure 2. The calculated E_{ads} values of molecules produced from carbohydrates are higher than those of molecules produced from lignin, which means phenol-based molecules produced from lignin have weaker interactions with the Ru catalyst than the furan-based molecules produced from carbohydrates. When furan-based molecules are present as an impurity alongside lignin, they competitively

Figure 1. Effects of sugars on lignin HDO conversion. a) Conversion of lignin and total yield of products. b) GC-MS of detectable products. c) Photographs showing difference in color of ethyl acetate extracts. Reaction conditions: In(OTf)$_3$ (0.1 mmol), Ru (0.05 mmol) as 5 wt% Ru/Al$_2$O$_3$, water (1.2 mL), $T=250$°C, $t=4$ h, $P_{H_2}=580$ psi. A: 100 mg lignin; B: 90 mg lignin + 10 mg glucose; C: 90 mg lignin + 10 mg xylose.

A= 100 mg lignin;

B=90 mg lignin+ 10 mg glucose;

C=90 mg lignin+ 10 mg xylose.

Figure 2. Calculated adsorption energies (E_{ads}) of molecules on Ru (0001) surface (a) and adsorption geometries of 5-HMF (b) and phenol (c) on Ru (0001) surface.
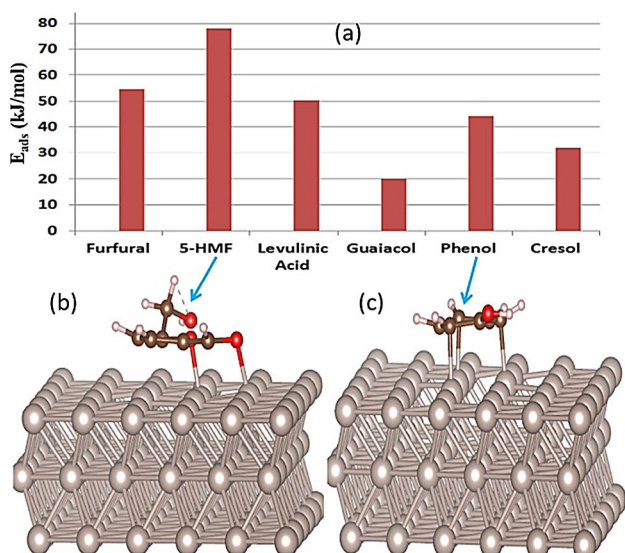
bind with the catalysts and thus reduce the interaction of phenol-based molecules with the catalysts, preventing further depolymerization and HDO conversion of lignin (Scheme 1). The results indicate that in furan-based molecules, mainly the O of the carboxyl group binds with the Ru (0001) surface (Figure 2b), whereas in phenol-based molecules, the C of the benzene ring binds with Ru surface (Figure 2c). The calculated O—Ru bond lengths in furan-based configurations are 0.1–0.2 Å shorter than the C—Ru bond lengths in phenol-based adsorption. These results indicate that the active sites of Ru (0001) surface are competitively occupied by furan-based molecules, blocking the phenol-based molecules from binding with the catalyst surface. Such poisoning effects caused by furans and their derivatives suppress lignin HDO conversion (Figure 1).

Thermogravimetric analysis (TGA) of the spent catalysts was also carried out to determine the carbon deposition on Ru/Al$_2$O$_3$ (Figure 3). These catalysts were collected from HDO reactions by using guaiacol, glucose, HMF, and furfural as reactants,
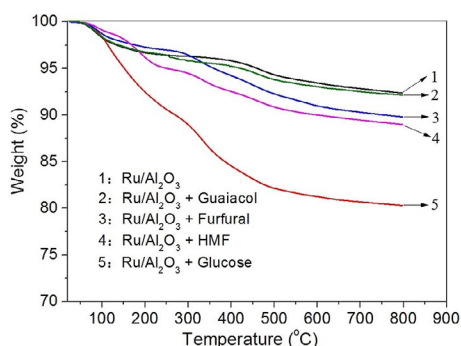
separately, under identical HDO reaction conditions. The conversion of these compounds, as well as the selectivity of products, were also analyzed. The dehydration of glucose to HMF was quite slow, and the yield of HMF and its hydrogenated products (mainly bishydroxymethyl tetrahydrofuran) was lower than 20%. Most of the glucose was converted into sorbitol (with a yield of 47%) under the reaction conditions, whereas the formation of char from glucose was significantly higher than that from other reactants, as indicated by TGA (Figure 3). Char or humins could be formed from glucose directly or from its dehydration intermediates. When HMF and furfural were used separately as reactants, the major products were found to be bishydroxymethyl tetrahydrofuran (with a yield of 63%) and hydroxymethyl tetrahydrofuran (with a yield of 76%), respectively. The formation of char from HMF and furfural is lower than that from glucose but higher than that from guaiacol (Figure 3). These results indicate that glucose, HMF, and furfural more easily form char or humins than guaiacol under the tested HDO reaction conditions. Char or humins from carbohydrates cover the metal surface of Ru/Al$_2$O$_3$ and deactivate the catalyst.

Conclusions

Valorization of biorefinery lignin-rich wastes improves the carbon efficiency of the entire process, this is an attractive but challenging topic for economic biorefinery design. Sugars and their derivatives (e.g., HMF) are present as impurities alongside lignin in biorefinery lignin-rich wastes. Negative effects of these compounds on lignin HDO conversion were found in this study. They could hinder lignin from hydrogenolysis depolymerization, as well as further preventing the formation of lignin depolymerization intermediates (monomers and dimers) through hydrogenation or deoxygenation. This mechanism was further validated by first-principles DFT calculations and thermogravimetric analysis of the spent catalysts. Compared with the acidic catalyst In(OTf)$_3$, the metal catalyst Ru/Al$_2$O$_3$ was more sensitive to sugars. The generated furan-based products and humins from sugars are responsible for the negative effects since these products can competitively absorb on the metal surface of catalysts and block the absorption of lignin and its degraded intermediates. The findings of this study suggest that the development of catalyst systems for lignin conversion should fully consider the influence of sugar impurities, and robust catalysts that are insensitive to sugars and their derivatives should be developed for effective lignin conversion.

Experimental Section

Chemicals and materials

All the chemicals used in this research are commercially available and used as received without any treatment. In(OTf)$_4$, glucose, xylose, HMF, cellulose (Avicel) were purchased from Sigma–Aldrich. Ru/Al$_2$O$_3$ (reduced) was purchased from Alfa Aesar. Lignin model compounds, including guaiacol, diphenyl ether, and benzyl phenyl ether, were purchased from Fisher Scientific. Lignin β-O-4 model compounds were purchased from GreenLignol, LLC. Lignin was ob-

Figure 3. Thermogravimetric analysis (TGA) of spent catalysts: 1. Fresh Ru/Al$_2$O$_3$; 2. Ru/Al$_2$O$_3$ after reaction with guaiacol; 3. Ru/Al$_2$O$_3$ after reaction with furfural; 4. Ru/Al$_2$O$_3$ after reaction with HMF; 5. Ru/Al$_2$O$_3$ after reaction with glucose.

tained from the National Renewable Energy Laboratory (NREL) by dilute alkali deacetylation and mechanical refining (DMR) treatment. All other chemicals were purchased from Fisher Scientific.

Hydrodeoxygenation of lignin model compounds and lignin

A known amount of lignin or lignin model compounds, catalysts, and water (1 mL or 1.2 mL) with or without sugar addition were added to a 3 mL dry glass sleeve. The sleeve was placed into a high-throughput batch reactor (PNNL-SA-117072, Bioproducts, Science & Engineering Laboratory). The reactor was sealed and purged with H_2 three times to exclude air, and then pressurized with 580 psi H_2 at room temperature. The reactor was heated to 250 °C and heating was maintained for 2 or 4 hours depending on the substrate. The metal plate of the high-throughput reactor was shaken (shaking frequency = 200 r min^{-1}) during the reaction to improve the mass transfer. After each run, the reactor was cooled to room temperature to terminate reactions. The glass sleeve was removed from the high-throughput reactor and the liquids were separated from the solids by centrifugation (8000 r min^{-1} for 10 min). The liquid was extracted with ethyl acetate (5 mL). The solids were also extracted with ethyl acetate (3 mL). The ethyl acetate extracts were combined and diluted in a 20 mL volumetric flask. Known amounts of vanillin and 3-methylheptane were added as internal standards for aromatics and hydrocarbons, respectively, in GC analysis.

Analysis of HDO products

The ethyl acetate-diluted liquid samples were analyzed by GC and GC-MS in an Agilent Technologies 7890A GC system with a DB-5 capillary column (30 m length × 250 µm I.D. × 0.25 µm film thickness, J&W Scientific) in the splitless mode. Typically, a 1 µl sample was injected with He (0.6 mL min^{-1}) as the carrier gas into the GC system. The injection port temperature was set at 300 °C. The GC oven was set to 45 °C and maintained for 6 min. Then the temperature was raised at a rate of 10 °C min^{-1} until it reached 300 °C and maintained at 300 °C for 2 min. Eluting compounds were detected with a MS (Agilent Technologies 5975C) inert XL EI/CI MSD with a triple axis detector, and compared by using NIST libraries. For model compounds, the reactant conversions and product selectivities were calculated by using the internal standard method based on the following formulae:

For the conversion of technical model compounds (HC = hydrocarbon):

$$\text{Conversion } \% = \frac{\text{Weight of reactant converted}}{\text{Weight of reactant added}} \times 100\% \quad (1)$$

$$\text{Yield of HC A } \% = \frac{\text{Carbon atoms in HC A}}{\text{Carbon atoms in reactant}} \times 100\% \quad (2)$$

$$\text{Sel. to HC A } \% = \frac{\text{Carbon atoms in HC A}}{\text{Total carbon atoms in products}} \times 100\% \quad (3)$$

For technical lignin, the calculations of conversion were based on the weight change of lignin before and after HDO reaction. The yield of lignin HDO products was calculated by the effective carbon number (ECN) approach.[31] 3-methylheptane was added as internal standard. The top 20 products were calculated to determine the total yield of HDO products.

For the conversion of technical lignin (HC = hydrocarbon):

$$\text{Conversion } \% = \frac{\text{Weight of reactant converted}}{\text{Weight of reactant added}} \times 100\% \quad (4)$$

$$\text{Yield of HC A } \% = \frac{\text{Weight of HC A produced}}{\text{Weight of reactant added}} \times 100\% \quad (5)$$

$$\text{Total HC yield} = \sum_{x=1}^{20} \text{Yield } x \quad (6)$$

DFT calculations

The calculations performed in this work are based on first-principles DFT with plane-wave basis sets and pseudopotentials to describe the electron–ion interactions. The Vienna ab initio simulation package (VASP, https://www.vasp.at) was employed to calculate molecule adsorption on the Ru (0001) surface. In this study, all calculations were done by using the PAW pseudopotentials and the PBE exchange-correlation functional. The plane-wave basis sets were used with a plane-wave cutoff energy of 500 eV and a kinetic energy cutoff for augmentation charges of 644.9 eV. The 6×6 Ru (0001) surface was created from optimized Ru crystal with space group P63/mmc (#194). To reduce the calculation cost, a three-layer Ru (0001) surface slab (108 atoms) with 20 Å vacuum separation was used in our calculation. Compared to the model in ref. [22], our model has larger surface area to eliminate the unexpected interactions between adsorbed molecules owing to periodicity. During adsorption calculations, the bottom layer of Ru was fixed as the bulk material, molecules were introduced on the surface for adsorption, and the lattice dimension was fixed. Except for the bottom layer of Ru, all atoms in the supercell were relaxed to the equilibrium configurations. 3×3×1 k-point sampling grids were applied in all adsorption calculations, whereas for pure molecule systems 4×4×4 k-point sampling grids were used. The valence electrons contain s and p orbitals for H, C, and O atoms and s, p, and d orbitals for Ru atoms. The adsorption energy (E_{ads}) is defined as $E_{ads} = (E_{Ru(0001)} + E_{Mol}) - E_{Ru-Mol}$, where E_{Ru-Mol}, $E_{Ru(0001)}$, and E_{Mol} are the DFT energies of the optimized molecule adsorbed on Ru (0001) surface slab, pure Ru (0001) surface slab, and the single molecule in a 20×20×20 Å supercell, respectively.

Hydrodeoxygenation reactions

HDO reactions of guaiacol, glucose, HMF, and furfural, separately, were conducted under identical reaction conditions, as listed in Table 1. To collect enough catalyst to carry out TGA, the scale of these reactions was magnified 5 times and reactions were carried out in a 10 mL batch reactor (5 mmol reactant, 0.25 mmol In(OTf)$_3$, 0.125 mmol Ru as 5 wt% Ru/Al$_2$O$_3$, 5 mL water as solvent). The conversions of glucose, HMF, and furfural, and the selectivities to generated products were analyzed by HPLC by using an external standard method.

Analysis of spent catalysts

The spent catalysts were subjected to thermogravimetric analysis (TGA) to determine carbon deposition after HDO reactions. All catalysts were collected after being reused three times, thoroughly washed with deionized water, and then dried at 65 °C before TGA testing. TGA was conducted with a Setaram Setsys thermogravimetric analyzer. The TG system was calibrated with calcium oxalate

monohydrate for temperature readings prior to experiments. In each run, approximately 5 mg of spent Ru/Al_2O_3 catalyst was put in an alumina crucible, and then the following experimental procedure was used: a) The TGA system was purged with N_2 for 10 min and then the furnace temperature was increased from room temperature to 30 °C at a heating rate of 1 °C min^{-1}; b) the temperature was held at 30 °C for 10 min and then ramped to the final temperature of 800 °C with a heating rate of 10 °C min^{-1} under the same atmosphere; c) when it reached the final temperature, the run was stopped and the temperature of the furnace was decreased to room temperature. Blank experiments were conducted by following the exact same procedure as above with an empty crucible to compensate for the output drift of the thermobalance. All experiments were carried out in duplicate.

Acknowledgements

Conflict of interest

The authors declare no conflict of interest.

[1] R. Rinaldi, R. Jastrzebski, M. T. Clough, J. Ralph, M. Kennema, P. C. Bruijnincx, B. M. Weckhuysen, *Angew. Chem. Int. Ed.* **2016**, *55*, 8164–8215; *Angew. Chem.* **2016**, *128*, 8296–8354.

[2] Z. Zhang, J. Song, B. Han, *Chem. Rev.* **2017**, *117*, 6834–6880.

[3] D. M. Alonso, S. H. Hakim, S. Zhou, W. Won, O. Hosseinaei, J. Tao, V. Garcia-Negron, A. H. Motagamwala, M. A. Mellmer, K. Huang, C. J. Houtman, N. Labbe, D. P. Harper, C. Maravelias, T. Runge, J. A. Dumesic, *Sci. Adv.* **2017**, *3*, e1603301.

[4] M. Kleinert, T. Barth, *Energy Fuels* **2008**, *22*, 1371–1379.

[5] M. P. Pandey, C. S. Kim, *Chem. Eng. Technol.* **2011**, *34*, 29–41.

[6] Y. He, X. Li, H. Ben, X. Xue, B. Yang, *ACS Sustainable Chem. Eng.* **2017**, *5*, 2302–2311.

[7] H. Wang, H. Ruan, H. Pei, H. Wang, X. Chen, M. P. Tucker, J. R. Cort, B. Yang, *Green Chem.* **2015**, *17*, 5131–5135.

[8] H. Wang, H. Wang, E. Kuhn, M. P. Tucker, B. Yang, *ChemSusChem* **2018**, *11*, 285–291.

[9] D. D. Laskar, B. Yang, H. Wang, J. Lee, *Biofuels Bioprod. Biorefin.* **2013**, *7*, 602–626.

[10] H. Wang, H. Ben, H. Ruan, L. Zhang, Y. Pu, M. Feng, A. J. Ragauskas, B. Yang, *ACS Sustainable Chem. Eng.* **2017**, *5*, 1824–1830.

[11] Z. Luo, Y. Wang, M. He, C. Zhao, *Green Chem.* **2016**, *18*, 433–441.

[12] J. Kong, B. Li, C. Zhao, *RSC Adv.* **2016**, *6*, 71940–71951.

[13] J. He, C. Zhao, J. A. Lercher, *J. Catal.* **2014**, *309*, 362–375.

[14] L. Shuai, M. T. Amiri, Y. M. Questell-Santiago, F. Héroguel, Y. Li, H. Kim, R. Meilan, C. Chapple, J. Ralph, J. S. Luterbacher, *Science* **2016**, *354*, 329–333.

[15] C. Li, X. Zhao, A. Wang, G. W. Huber, T. Zhang, *Chem. Rev.* **2015**, *115*, 11559–11624.

[16] C. P. Xu, R. A. D. Arancon, J. Labidi, R. Luque, *Chem. Soc. Rev.* **2014**, *43*, 7485–7500.

[17] J. Zakzeski, P. C. A. Bruijnincx, A. L. Jongerius, B. M. Weckhuysen, *Chem. Rev.* **2010**, *110*, 3552–3599.

[18] R. Shu, J. Long, Y. Xu, L. Ma, Q. Zhang, T. Wang, C. Wang, Z. Yuan, Q. Wu, *Bioresour. Technol.* **2016**, *200*, 14–22.

[19] S. Constant, H. L. Wienk, A. E. Frissen, P. de Peinder, R. Boelens, D. S. van Es, R. J. Grisel, B. M. Weckhuysen, W. J. Huijgen, R. J. Gosselink, *Green Chem.* **2016**, *18*, 2651–2665.

[20] F. P. Bouxin, A. McVeigh, F. Tran, N. J. Westwood, M. C. Jarvis, S. D. Jackson, *Green Chem.* **2015**, *17*, 1235–1242.

[21] C. Chesi, I. B. de Castro, M. T. Clough, P. Ferrini, R. Rinaldi, *ChemCatChem* **2016**, *8*, 2079–2088.

[22] A. A. Dwiatmoko, S. Lee, H. C. Ham, J.-W. Choi, D. J. Suh, J.-M. Ha, *ACS Catal.* **2015**, *5*, 433–437.

[23] X. Chen, W. Wang, P. Ciesielski, O. Trass, S. Park, L. Tao, M. P. Tucker, *ACS Sustainable Chem. Eng.* **2016**, *4*, 324–333.

[24] C. Zhao, J. A. Lercher, *ChemCatChem* **2012**, *4*, 64–68.

[25] S. Kobayashi, K. Manabe, *Acc. Chem. Res.* **2002**, *35*, 209–217.

[26] H. Wang, M. Feng, B. Yang, *Green Chem.* **2017**, *19*, 1668–1673.

[27] G. Yao, G. Wu, W. Dai, N. Guan, L. Li, *Fuel* **2015**, *150*, 175–183.

[28] A. Kloekhorst, H. J. Heeres, *ACS Sustainable Chem. Eng.* **2015**, *3*, 1905–1914.

[29] J. Zhang, J. Teo, X. Chen, H. Asakura, T. Tanaka, K. Teramura, N. Yan, *ACS Catal.* **2014**, *4*, 1574–1583.

[30] B. J. Arena, *Appl. Catal. A* **1992**, *87*, 219–229.

[31] J. T. Scanlon, D. E. Willis, *J. Chromatogr. Sci.* **1985**, *23*, 333–340.